Longevity mutation in *SCH9* prevents recombination errors and premature genomic instability in a Werner/Bloom model system

Federica Madia,[1] Cristina Gattazzo,[1] Min Wei,[1] Paola Fabrizio,[1] William C. Burhans,[2] Martin Weinberger,[2] Abdoulaye Galbani,[1] Jesse R. Smith,[1] Christopher Nguyen,[1] Selina Huey,[1] Lucio Comai,[3] and Valter D. Longo[1]

[1]Andrus Gerontology Center and Department of Biological Sciences, University of Southern California, Los Angeles, CA 90089
[2]Department of Cell Stress Biology, Roswell Park Cancer Institute, Buffalo, NY 14263
[3]Institute of Genetic Medicine, Keck School of Medicine, University of Southern California, Los Angeles, CA 90033

Werner and Bloom syndromes are human diseases characterized by premature age-related defects including elevated cancer incidence. Using a novel *Saccharomyces cerevisiae* model system for aging and cancer, we show that cells lacking the RecQ helicase *SGS1* (WRN and BLM homologue) undergo premature age-related changes, including reduced life span under stress and calorie restriction (CR), G1 arrest defects, dedifferentiation, elevated recombination errors, and age-dependent increase in DNA mutations. Lack of *SGS1* results in a 110-fold increase in gross chromosomal rearrangement frequency during aging of nondividing cells compared with that generated during the initial population expansion. This underscores the central role of aging in genomic instability. The deletion of *SCH9* (homologous to AKT and S6K), but not CR, protects against the age-dependent defects in *sgs1*Δ by inhibiting error-prone recombination and preventing DNA damage and dedifferentiation. The conserved function of Akt/S6k homologues in lifespan regulation raises the possibility that modulation of the IGF-I–Akt–56K pathway can protect against premature aging syndromes in mammals.

Introduction

Sgs1 is the only known *Saccharomyces cerevisiae* member of the RecQ helicase family of DNA unwinding proteins, which is involved in the maintenance of genomic stability in organisms ranging from *Escherichia coli* to humans. Mutations in at least three of the five human genes encoding RecQ helicases (BLM, WRN, and RECQ4) promote genomic instability and cancer. Specific mutations in BLM cause Bloom's Syndrome (BS), which is characterized by increased sister chromatid exchanges and a wide variety of tumors, as well as diabetes and immunodeficiency (Hickson et al., 2001; Mohaghegh and Hickson, 2002; Thompson and Schild, 2002; Kaneko and Kondo, 2004). WRN mutations, which cause Werner's syndrome (WS), promote cancer, cardiovascular diseases, diabetes, and immunodeficiency and accelerate other age-related changes, including graying of the hair, wrinkling of the skin, and osteoporosis (Epstein et al., 1966; Ozgenc and Loeb, 2005). The first connection between the yeast WRN/BLM homologue and premature aging was demonstrated by the fact that mutants lacking *SGS1* showed a shortened replicative life span (Sinclair et al., 1997). Furthermore, expression of either human BLM or WRN gene in yeast was able to suppress certain recombination phenotypes of yeast lacking *SGS1* (Yamagata et al., 1998), indicating that these human genes are, at least in part, functional homologues of *SGS1*. Sgs1 is required to prevent defective DNA recombination, which causes premature G2/M arrest and senescence (Johnson et al., 2001; McVey et al., 2001). RecQ helicases catalyze the DNA unwinding through the conserved RecQ domain, which was originally described for the *E. Coli* RecQ protein (Gangloff et al., 1994; Sun et al., 1999). In the *S. cerevisiae* Sgs1 (1,447 aa), the RecQ domain is followed, as in most of the RecQ proteins, by a RecQ C-terminal domain (a C-terminal extension from the helicase domain, which is involved in protein–protein interactions) and the HRCD domain (helicase/RNase D

F. Madia and C. Gattazzo contributed equally to this paper.

Correspondence to Valter D. Longo: vlongo@usc.edu

Abbreviations used in this paper: 5FOA, 5-fluoroorotic acid; BS, Bloom's Syndrome; CFU, colony-forming unit; CLS, chronological life span; CR, calorie restriction; GCR, gross chromosomal rearrangement; IR, inverted repeat; MMS, methyl methane sulfonate; NHEJ, nonhomologous end joining; SDC, synthetic dextrose complete; WS, Werner's Syndrome; YPD, yeast extract peptone dextrose medium.

The online version of this paper contains supplemental material.

The Journal of Cell Biology, Vol. 180, No. 1, January 14, 2008 67–81
http://www.jcb.org/cgi/doi/10.1083/jcb.200707154

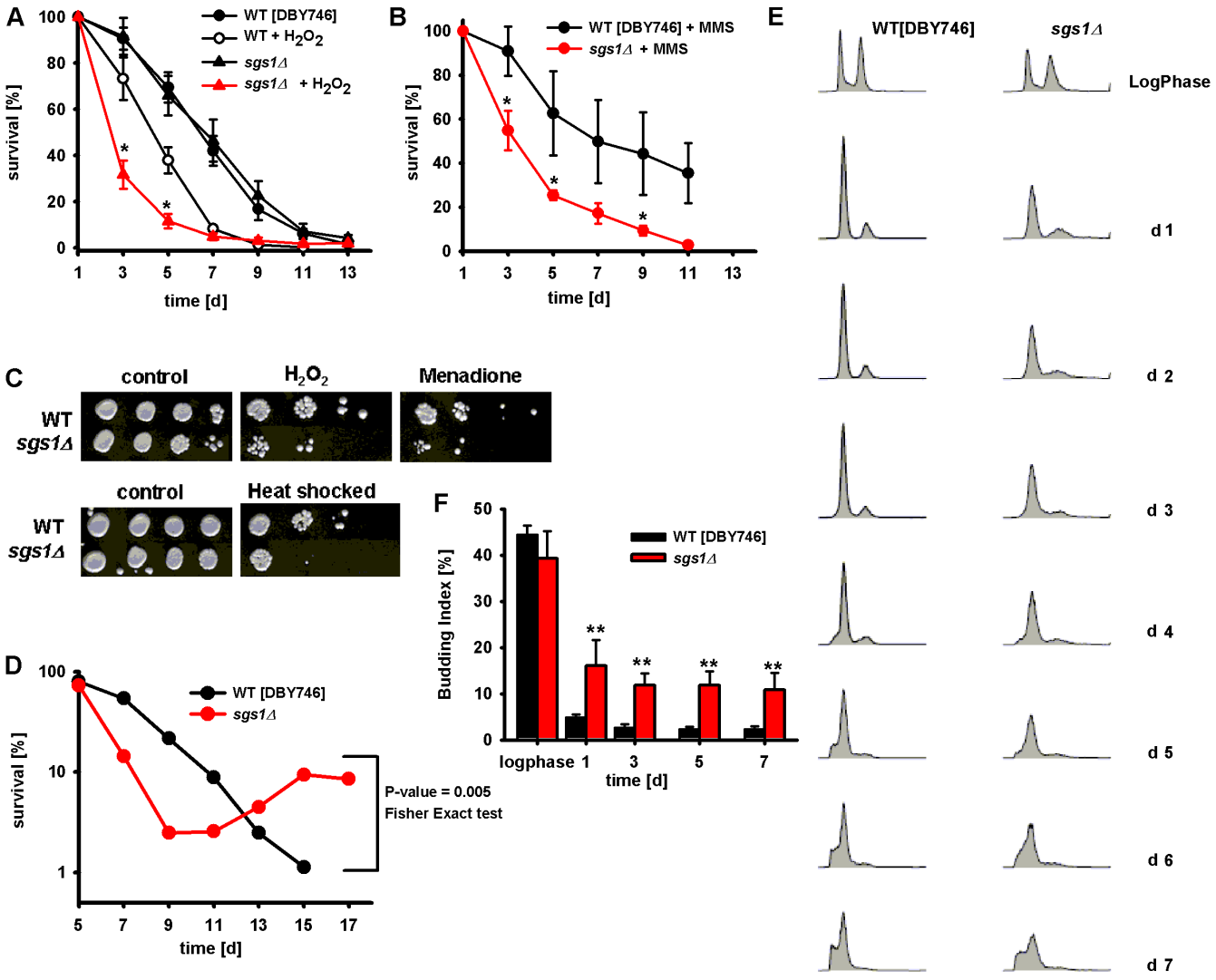

Figure 1. **Chronological survival of *sgs1Δ* mutants.** (A and B) Chronological survival in synthetic complete medium (SDC) of wild-type (DBY746) and *sgs1Δ* mutant cells in standard conditions or after chronic exposure (days 1 and 3) to either 1 mM H_2O_2 (A) or 0.001% MMS (B). Data represent the mean ± SEM (n = 12–17). *, P < 0.05 (*sgs1Δ* treated cells vs. wild-type treated cells). (C) Oxidative stress and heat shock resistance of wild-type and *sgs1Δ* mutant. Day-3 cells were exposed to 100 mM H_2O_2 for 30 min, 250 μM menadione for 60 min (top), or heat shock treatment at 55°C for 90 min (bottom). These experiments were repeated three times with similar results. (D) Survival and regrowth/dedifferentiation during the high mortality phase (day 7–17) of wild-type and *sgs1Δ* mutant. A representative experiment is shown (see Table I). (E) Cell-cycle profiles of wild-type (DBY746) and *sgs1Δ* mutant cells during log phase and from day 1–7. (F) Budding index of wild-type and *sgs1Δ* mutant cells. Data represent the mean ± SEM (n = 7–8). **, P < 0.01 (*sgs1Δ* cells vs. wild-type cells).

C terminal, which is involved in DNA binding). Moreover, Sgs1 contains key domains, including one required for S-phase checkpoint function and others that interact with Top3, Rad51, or checkpoint kinase Rad53 (Miyajima et al., 2000b; Mullen et al., 2000; Onodera et al., 2002; Ui et al., 2005). The structural complexity of this protein may explain the multiplicity of cellular processes in which Sgs1 is involved (S-phase checkpoint, replication, double-strand break repair, recombination, telomere maintenance, etc.), as well as the complexity of phenotypes associated with its deficiency (Bennett and Keck, 2004; Cobb and Bjergbaek, 2006; Killoran and Keck, 2006).

The helicase and Top3 interaction domains, but not the S-phase checkpoint function domain, were shown to be required to prevent rapid clonal senescence in *S. cerevisiae* telomerase mutants. This was measured by monitoring population doublings (Azam et al., 2006). The Sgs1–Top3 complex has also been implicated in interactions with mismatch repair proteins (Myung et al., 2001). Because mismatch proteins act to limit recombination between similar, but not identical, DNA sequences, it is possible that RecQ proteins also act to limit recombination by reversing inappropriate heteroduplex intermediates. In fact, hMSH2/6 forms a complex with human BLM–p53–RAD51 in response to the damaged DNA forks during double-stranded–break repair (Pedrazzi et al., 2003; Yang et al., 2004). The hyper-recombination and erroneous (homeologous) recombination seen in *sgs1Δ* cells appear to play a central role in the high level of gross chromosomal rearrangements (GCRs) observed in these mutant strains (Onoda et al., 2000; Myung et al., 2001; Myung and Kolodner, 2002; Schmidt et al., 2006). Sister chromatid exchange and exchange of genetic material between different

Table I. **Percentage of age-dependent early dedifferentiation (days 7–17)**

Background	Strains		
	Wild type % (n)	*sgs1Δ* % (n)	*sch9Δ sgs1Δ* % (n)
DBY746	8.0 (38)	47.4 (38)[a]	12.0 (25)[b]
BY4741	16.7 (6)	50.0 (6)	0.0 (6)
SP1	66.7 (3)	100.0 (3)	0.0 (3)

[a]P = 0.005 (vs. wild type; Fisher's exact test).
[b]P = 0.036 (vs. *sgs1Δ*; Fisher's exact test).

Table II. **Percentage of cells in each cell-cycle compartment at early time points**

Time point	Cell-cycle phase	Strain		
		Wild type (DBY746)	*sgs1Δ*	*sch9Δ sgs1Δ*
Log phase	*sub G1*	0.0	0.6	0.4
	G1	31.5	35.2	59.4
	S	16.6	11.8	3.0
	G2/M	51.9	52.9	37.6
Day 1	*sub G1*	0.3	0.3	0.0
	G1	82.0	69.5	71.7
	S	0.0	4.0	12.3
	G2/M	18.0	26.4	15.6
Day 2	*sub G1*	0.4	0.2	0.0
	G1	82.5	68.8	86.9
	S	1.5	12.6	7.5
	G2/M	16.0	18.5	5.7
Day 3	*sub G1*	2.9	2.0	0.0
	G1	79.4	72.9	86.6
	S	7.8	14.0	9.3
	G2/M	12.7	13.1	4.1

Data are from FACS analysis measurements presented in Figs. 1 E and 5 B and calculated using MODFIT.

chromosomes may be important features of RecQ helicase deficiency because they are commonly observed in human BS cells (Ellis et al., 1995; German, 1995). WS cells do not show an elevated sister chromatid–exchange frequency, but they do display increased illegitimate recombination and a high frequency of large chromosomal deletions (Shen and Loeb, 2000).

In this paper, we develop a simple yeast system modeling BS and WS, based on studies of the chronological life span (CLS) and on the monitoring of cell-cycle profile, DNA mutations, chromosomal rearrangements, and dedifferentiation of *sgs1Δ* mutants during chronological aging. Using this model system, we describe a marked age-dependent increase in various categories of mutations in cells lacking *SGS1,* which can be prevented by the deletion of *SCH9*, a homologue of mammalian *AKT* and S6 kinase (Toda et al., 1988; Urban et al., 2007). We provide evidence that points to enhanced cellular protection against stress, tighter G1 arrest, and reduced recombination errors as mechanisms by which lack of Sch9 activity protects against genomic instability and dedifferentiation associated with accelerated aging in *sgs1Δ* mutants.

Results

Aging in *sgs1Δ* mutants

Yeast *sgs1Δ* of three different genetic backgrounds (DBY746, BY4741, and SP1) did not have a shortened CLS when maintained in standard glucose/ethanol-containing medium (Fig. 1 A and Fig. S1, available at http://www.jcb.org/cgi/content/full/jcb.200707154/DC1). This observation was confirmed by measuring CLS using the phloxin B live/dead staining (Kucsera et al., 2000), which ruled out the possibility that wild-type cells may live longer than *sgs1Δ* mutants but may be unable to form a colony. However, premature death was observed after chronic exposure of *sgs1Δ* mutants to either hydrogen peroxide or the alkylating agent methyl methane sulfonate (MMS; Fig. 1, A and B). Sgs1-deficient cells aging chronologically were also hypersensitive to acute heat shock or acute treatment with hydrogen peroxide or the superoxide/H_2O_2-generating agent menadione (Fig. 1 C).

Increased chronological age-dependent dedifferentiation and G1 arrest defects in yeast *sgs1Δ* mutants

We have previously shown that yeast mutants reminiscent of cancer cells, which dedifferentiate and grow by using the nutrients released by dead cells, can emerge within aging *S. cerevisiae* cultures (Fabrizio et al., 2004). The frequency of this phenotype was doubled in cells lacking cytosolic superoxide dismutase 1 and greatly reduced in long-lived mutants or mutants overexpressing superoxide dismutases (Fabrizio et al., 2004). Because both WS and BS are associated with elevated age-dependent cancer incidence, we tested whether mutations in *SGS1* affected this dedifferentiation phenotype. Subpopulations of cells were considered to be dedifferentiating/regrowing if the viability counts during the high mortality phase (days 7–17) either increased by at least 50% or did not decrease in three consecutive counts (6 d) as expected, based on the normal age-dependent exponential increase in mortality rates (Finch, 1990). Early dedifferentiation occurred in 3 out of 38 wild-type DBY746 cultures but in 18 out of 38 *sgs1Δ* cultures (48%; P = 0.005 [Fisher's exact test]; Fig. 1 D and Table I). The frequency of dedifferentiation in wild-type cells was lower than that reported in our previous study (Fabrizio et al., 2004) because dedifferentiation after day 17 was not considered. Similarly, in the SP1 genetic background, early dedifferentiation occurred in two out of three wild-type cultures (67%) and three out of three *sgs1Δ* cultures (100%), and in the BY4741 background in one out of six wild-types cultures (17%) but three out of six *sgs1Δ* cultures (50%; Table I). These results suggest that Sgs1 contributes to the prevention of age-dependent dedifferentiation.

To further test the hypothesis that Sgs1 might exert a role in blocking cellular dedifferentiation, we determined cell-cycle and budding index profiles during aging. FACS analysis showed a similar profile for both log-phase wild-type and *sgs1Δ* mutant cells (Fig. 1 E and Table II). Starting on day 1, wild-type cells were mostly G1 arrested with only 5% of cells with small buds (Fig. 1 F), and a lower percentage of cells were in S phase (Table II). The efficiency of G1 arrest is indicated by the increased height and narrowness of the G1-DNA content

peak and the smaller amount of cells with an S-phase or G2/M content of DNA. In accordance with the dedifferentiation phenotype showed by the Sgs1-deficient strain (Fig. 1 D), *sgs1Δ* mutant cultures displayed a slightly lower G1 arrest than wild-type cells but a threefold increase in budding index (15%) and a 2–10-fold higher percentage of cells in S phase (Fig. 1, E and F; and Table II).

Premature genomic instability in *sgs1Δ* mutants

To characterize the type of DNA damage occurring during normal and premature aging (Lombard et al., 2005), we monitored the frequency of Can^r mutations, GCRs, base substitutions (*trp1-289* reversions, *trp*$^-$→*TRP1*$^+$), and small DNA insertions/deletions (*lys2-Bgl*→*LYS*$^+$; Madia et al., 2007) in both wild-type and Sgs1-deficient *S. cerevisiae* aging chronologically (Fig. S2, available at http://www.jcb.org/cgi/content/full/jcb.200707154/DC1). Can^r mutations impart cellular resistance to the arginine analogue canavanine (L-canavanine sulfate) and are easily detectable. During growth, they are mostly caused by a combination of frameshifts and point mutations in the *CAN1* gene (Chen et al., 1998). In our previous papers, we showed that in the wild-type DBY746 genetic background, spontaneous Can^r mutations increased progressively with age and reached a frequency of approximately three to five per one million cells by day 11–13 (Fig. 2 A; Fabrizio et al., 2004, 2005). Similar to what had been shown in growing yeast cells (Myung et al., 2001), mutations in *SGS1* did not induce an increase of Can^r frequency on day 1 of a chronological aging study compared with the wild-type strain (Fig. 2 A). However, the frequency increased rapidly in *sgs1Δ* mutants and reached a threefold higher level than in wild-type cells by days 7 and 9 (Fig. 2 A). An analogous, but delayed, effect on Can^r mutations was observed in the longer-lived BY4741 genetic background (Fig. S3 A).

To gain further insight into the type of age-dependent mutations, we analyzed the spectra of mutations in 10 Can^r mutant colonies from 7-d-old *sgs1Δ* mutant cultures (Table III). We were only able to PCR amplify and sequence the entire *CAN1* gene in 5 out of 10 Can^r mutants from 7-d-old *sgs1Δ* cultures (Table III), which suggests that half of the *CAN1* genes contain GCRs that prevent sequencing. Sequencing of the *CAN1* gene revealed that four mutants carried a single point mutation (three with base substitution and one with deletion) and one a double mutation (Table III). The four-base substitutions were C→A transversions (two of four) and T→C transitions (two of four), whereas the deletions were ΔA and ΔT (Table III). Thus, in addition to suppressing GCRs during growth (Myung et al., 2001; Myung and Kolodner, 2002), Sgs1 protects against GCRs and, possibly, other mutations during chronological aging.

Kolodner and co-workers had shown, during the growth phase, a 20-fold increase in the rate of GCRs in *sgs1Δ* mutants when compared with wild-type yeast (Myung et al., 2001; Myung and Kolodner, 2002). We measured the GCR frequency in log-phase (OD_{600} of ∼1) wild-type and Sgs1-deficient cultures and obtained similar results (wild type, $0.51 \pm 0.03 \times 10^{-8}$ cells; *sgs1Δ*, $8.20 \pm 0.45 \times 10^{-8}$ cells). During chronological aging, the frequency of GCRs underwent a 40-fold age-dependent increase in wild-type cells and a 110-fold increase in the *sgs1Δ* mutant between days 1 and 13 (Fig. 2 B), underscoring the central role of aging in genomic instability. It should be noted that this increase in GCR frequency was observed on day 13 when <5% of the initial population was still alive. Thus, it represents a very high genomic instability in the subpopulation that survives until day 13. The GCR results are in agreement with the inability to totally or partially PCR amplify the *CAN1* gene in half of the Can^r mutants that emerged from *sgs1Δ* cultures (Table III).

Point and insertion/deletion mutations in *sgs1Δ* mutants

As an additional method to monitor the occurrence of point mutations in cells aging chronologically, we measured the frequency of age-dependent C→T base substitutions, which cause reversion of the *trp1-289* amber mutation present in the DBY746 genetic background and allow growth in the absence of tryptophan (Fig. S2). The frequency of *trp1-289* reversion mutation was similar between wild-type and *sgs1Δ* mutants between days 3 and 9 and was significantly lower in *sgs1Δ* mutants compared with that in wild-type cells at day 11 (Fig. 2 C). These results were in agreement with the absence of C→T base substitutions in the sequenced *CAN1* genes (Table III).

To further characterize the link between Sgs1 and the age-dependent mutations and as an indirect measure of nonhomologous end-joining (NHEJ) repair (Heidenreich et al., 2003), we examined how lack of Sgs1 affected the frequency of small insertions of 2 or 5 bp or deletions of 1 or 4 bp, which cause a frameshift and allow the expression of Lys2 (Fig. S2). We monitored the frequency of reversion of the lysine auxotrophy phenotype of a *lys2-Bgl* mutant aging chronologically (Boulton and Jackson, 1996; Heidenreich et al., 2003). Although the frequency of *LYS*$^+$ mutations was similar in young wild-type and *sgs1Δ* mutants, it increased by 13-fold in wild-type cells but only sixfold in *sgs1Δ* mutants by day 11. The sequencing of the mutated *CAN1* gene from *sgs1Δ* mutants at day 7 confirmed that the frequency of small insertions/deletions was reduced (Table III). Collectively, these data indicate that C→T substitutions and NHEJ-dependent insertions/deletions occur at a normal or reduced rate in *SGS1*-deficient yeast (Fig. 2, C and D; and Table III).

Role of Sgs1 functional domains in age-dependent genomic instability

The characterization of the yeast *SGS1* gene indicated that different *SGS1* domains have distinct functions (Miyajima et al., 2000a,b; Mullen et al., 2000; Lo et al., 2006). As a first step toward mapping the different Sgs1 domains required for age-dependent mutation and dedifferentiation avoidance, we generated yeast strains lacking either the region encoding for the C-terminal 200 aa (*sgs1-ΔC200*) or the N-terminal 50 aa (*sgs1-ΔN50)* or bearing a mutation that disrupts the helicase activity (*sgs1-hd*) by a single amino acid change within the ATP binding domain of Sgs1 (K706A; Mullen et al., 2000; Azam et al., 2006). The mutated, as well as the wild-type, *SGS1* alleles (*sgs1Δ-SGS1*) were integrated at the *LEU2* locus of *sgs1Δ* mutant. Chronological survival

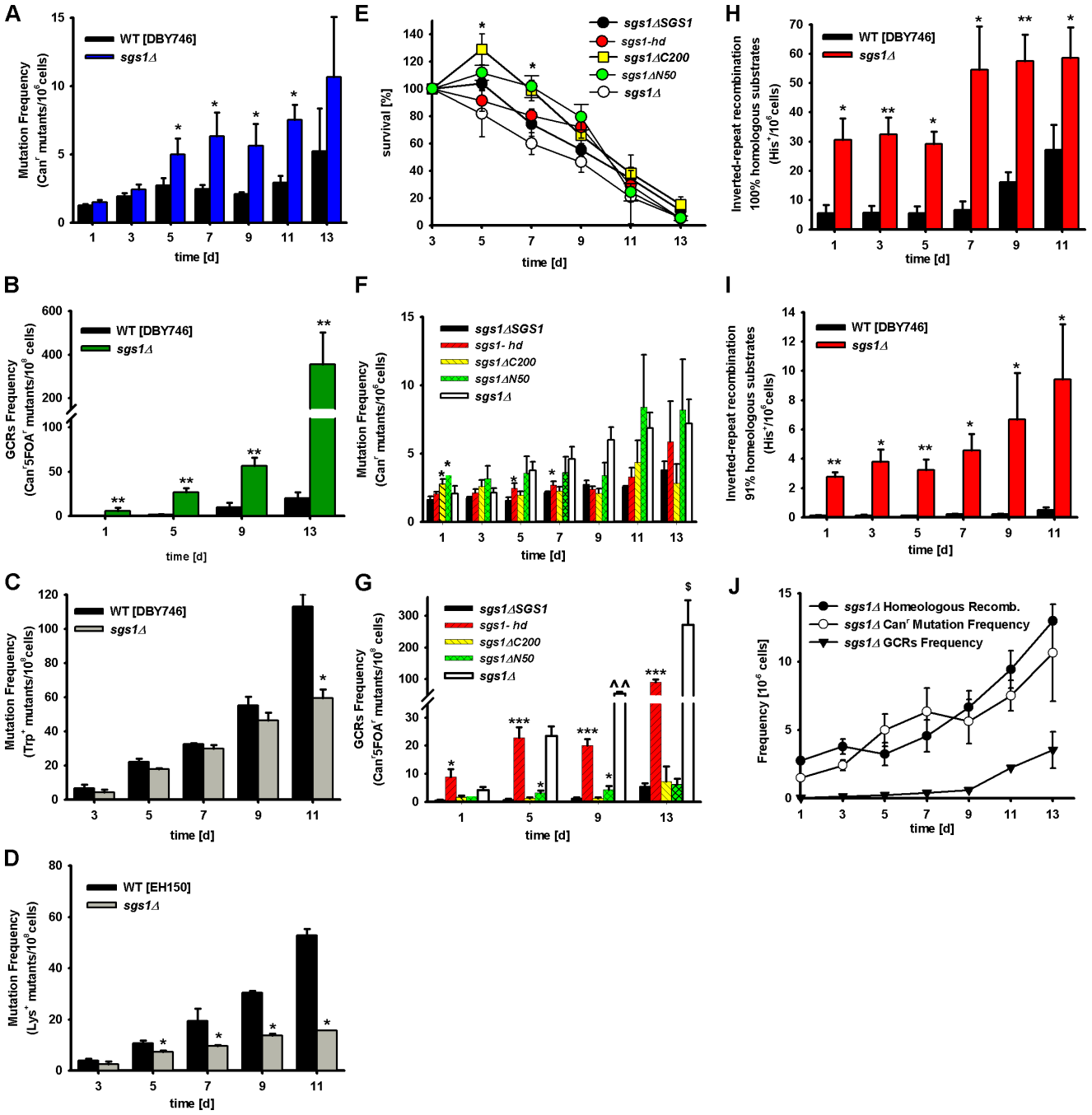

Figure 2. **Premature genomic instability in *sgs1Δ* mutants.** (A) Age-dependent mutation frequency in *CAN1* gene, measured as Can^r mutants/10^6 cells of wild-type (DBY746) and *sgs1Δ* cells. The mean ± SEM is shown (n = 12–16). (B) Age-dependent GCR frequency measured as Can^{r}5FOA^r mutants/10^8 cells, in *sgs1Δ* mutants compared with wild-type cells. The mean ± SEM is shown (n = 7–11). (C) Age-dependent spontaneous base-substitution mutations measured as tryptophan reversions in wild-type and *sgs1Δ* mutant. Data are presented as mean ± SEM. (D) Age-dependent spontaneous small insertion/deletion mutations measured as Lys$^+$ revertants in the EH150 genetic background. Mutation frequencies over time were measured as cumulative appearance of Trp$^+$ or Lys$^+$/10^8 cells. The means ± SEM are presented (n = 6–9). (E–G) Survival (E) of mutants carrying *sgs1Δ*, *sgs1-ΔC200*, *sgs1-ΔN50*, *sgs1-hd* alleles, and *sgs1ΔSGS1* in DBY746 background and age-dependent mutation frequency of Can^r mutants (F) and GCRs (G). The means ± SEM are shown (n = 7–8). (H and I) Age-dependent homologous (H) and homeologous (I) recombination frequency measured as His$^+$/10^6 cells of wild-type and *sgs1Δ* mutant cells. Data are shown as mean ± SEM (n = 4). (J) Age-dependent homeologous recombination events, Can^r mutation, and GCR frequencies per million cells in the DBY746 strain lacking *SGS1*. Data are presented as mean ± SEM. *, P < 0.05; **, P < 0.01; ***, P < 0.001 (vs. wild type). ^, P < 0.05; ^^, P < 0.01 (*sgs1Δ* vs. *sgs1-hd*).

assay, Can^r mutation frequency, and GCR frequency assays were performed with these strains.

Yeast strains lacking the helicase domain (*sgs1-hd*) or the N-terminal 50-aa region (*sgs1-ΔN50*) showed no difference in survival when compared with the strain lacking the entire protein (*sgs1Δ*) or the wild type (Fig. 2 E). Notably, the cell density of yeast lacking the S-phase checkpoint domain (*sgs1-ΔC200*) continued to increase slightly until day 5 (Fig. 2 E), which is in

Table III. **Spectrum of mutations observed in Can^r colonies from day 7**

Clone	*Mutation type*			*Position from ATG*	*Sequence*
Wild type[a]					
1	Base substitution	C→T	Proline-leucine	656	TGTTCC**C**TGTC
2	Base substitution	T→G	Asparagine-lysine	1173	AAA**T**TCAAATA
	Insertion	G		1710	GAGGC-G-AATTGT
3	Duplication		248bp	184–431	
4	Base substitution	G→C	Alanine-proline	709	TTTTA**G**CCATTA
	Deletion	TG	Isoleucine-arginine frameshift	1098–1099	TTGCTATTGAGAA
5	Base substitution	G→T	Glycine-valine	353	ACGCCG**G**CCCAG
	Insertion	A		1341	CAAA-A-GTTTTCG
6	Base substitution	C→T	Proline-serine	937	GCTGCAAAC**C**CCA
7	*no PCR*				
8	Deletion	AT	Frameshift	1129–1130	TGTCACATATCTT
	Insertion	T	Frameshift (T_3-T_4)	1086	CCCTTT-T-ATTATT
9	Base substitution	G→T	Tryptophan-cysteine	531	GGTTTTCTTG**G**CA
	Deletion	A	Frame-shift (A_3-A_2)	663	CAAATATTACGGT
	Insertion	T	Frameshift (T_3-T_4)	1086	CCCTTT-T-ATTATT
10	Base substitution	G→A	Glutamic acid-lysine	679	GAATTC**G**AGTTCT
	Base substitution	G→T	Valine-phenylalanine	907	GAACTA**T**TTGGTA
	Deletion	A	Frameshift	1217	TATCAAAGAACAC
sgs1Δ[b]					
1	Base substitution	C→A	Tyrosine-STOP	591	GGACGTA**C**AAAG
	Deletion	A	Frameshift (A_6-A_5)	969	TCAAAAAAGTTGC
2	Deletion	T	Frameshift	1756	GAATGTTGTAGC
3	*partially sequenced*				
4	*no PCR*				
5	Base substitution	T→C	Valine-alanine	659	GTTCCCTG**T**CAAA
6	*no PCR*				
7	*partially sequenced*				
8	*no PCR*				
9	Base substitution	T→C	Tryptophan-arginine	529	GGTTTTCT**T**GGGC
10	Base substitution	C→A	Alanine-aspartic acid	1166	ATTTCTG**C**CGCAA
sch9Δsgs1Δ[c]					
1	Insertion	CT	Frameshift	1006–1007	GCTCTCT-CT-ATT
2	Base substitution	G→A	Glycine-serine	670	ATTAC**G**GTGAATT
3	Base substitution	G→T	Glutamic acid-STOP	184	TGGC**G**AGGATAC
4	*partially sequenced*				
5	*no PCR*				
6	Base substitution	A→C	Tyrosine-serine	1184	TATTT**A**CGTTGGT
7	Base substitution	G→T	Glycine-valine	911	TAGTTG**G**TATCAC
8	Base substitution	G→A	Glycine-serine	922	ACTGCTG**G**TGAAG
9	Base substitution	C→A	Phenylalan-leucine	1193	ACGTTGGTT**C**CTA
10	Deletion	T	Frameshift leucine-phenyalan	543	AATCACTTTTGCC
	Base substitution	G→C	No change	544	AATCACTTTT**G**CC

Base substitutions: bold, insertions; underline, deletions.
[a]Total clones: 10 (no PCR, 1/10; sequenced, 9/10).
[b]Total clones: 10 (no PCR, 3/10; partially sequenced, 2/10; sequenced, 5/10).
[c]Total clones: 10 (no PCR, 1/10; partially sequenced, 1/10; sequenced, 8/10).

agreement with a helicase-independent role for the Sgs1 S-phase domain in regulating G1 arrest and dedifferentiation during aging. Because this growth effect was not observed in *sgs1Δ*, it appears that the lack of the checkpoint domain in cells that otherwise maintain other functions is more permissive to the observed additional 20% growth. Lack of the S-phase checkpoint function did not affect the age-dependent Can^r mutation frequency (Fig. 2 F). However, at day 1, *sgs1-ΔC200* cells displayed a significantly higher mutation frequency compared with the wild type (*sgs1-ΔC200*, $2.75 \pm 0.38 \times 10^{-6}$; *sgs1ΔSGS1*, $1.62 \pm 0.26 \times 10^{-6}$; $P < 0.05$), indicating that the sgs1-*ΔC200* cells have a slightly higher mutation rate during growth (Fig. 2 F). The mutated Sgs1 bearing a deletion in the N-terminal 50 aa (*sgs1-ΔN50)* lacks residues that are essential for the interaction with Top3, a type I topoisomerase that cooperates with Sgs1p during homologous recombination (Bennett and Wang, 2001;

Fabre et al., 2002; Onodera et al., 2002). The age-dependent mutation frequency (Can^r) of the *sgs1-ΔN50* mutant was also elevated on day 1 (Fig. 2 F; *sgs1-ΔN50*, $3.40 \pm 0.74 \times 10^{-6}$; *sgs1ΔSGS1*, $1.62 \pm 0.26 \times 10^{-6}$; $P < 0.05$) but did not display a significant age-dependent increase when compared with *sgs1ΔSGS1* cells (Fig. 2 F). Similar Can^r frequency results were obtained with the *sgs1-hd* allele, which carries a single point mutation in the helicase domain and has no detectable DNA helicase activity (Mullen et al., 2000; Fig. 2 F).

Our data indicate that only the combination of various activities of the Sgs1 protein completely protects against age-dependent Can^r mutations. These activities may include some that we have not investigated or remain unknown. In contrast, the DNA helicase activity appears to be involved in the avoidance of a major portion of GCRs during aging (Fig. 2 G). Until day 5 of a standard chronological aging study, the *sgs1-hd* allele showed a similar GCR frequency compared with that of *sgs1Δ* mutants. At days 9 and 13, the Sgs1-deficient strain showed a two- to threefold higher GCR frequency compared with *sgs1-hd*. These results suggest that the helicase activity of Sgs1 plays a central role in the avoidance of age-dependent GCRs but that other domains of Sgs1 also protect against gross chromosomal damage.

Hyperhomologous and homeologous recombination in aging *sgs1Δ* mutants

To determine whether erroneous recombination, previously shown to play a major role in GCR occurrence during growth in *sgs1Δ* mutants (Myung et al., 2001), might be responsible for both Can^r mutations and GCRs during aging, we measured the frequency of homologous and homeologous recombinational events in wild-type and Sgs1-deficient strains. We generated wild-type DBY746 and *sgs1Δ* mutants in which we could measure the frequency of recombination between inverted-repeat substrates with 100 or 91% homology, as described previously (Datta et al., 1996). Both homologous and homeologous recombination were much higher in *sgs1Δ* mutants compared with wild-type cells on day 1 (end of the growth phase; Fig. 2, H and I). During chronological aging, the frequency of homologous recombinational events remained stable up to day 5 and then increased by two to threefold in both wild-type and *sgs1Δ* cells. Homeologous recombination frequency increased steadily between days 5 and 11 in both wild-type cells and *sgs1Δ* mutants (Fig. 2, H and I). The maximum difference between *sgs1Δ* mutants and wild-type cells was observed by day 5–7 with the *sgs1Δ*/wild-type ratio reaching 8- and 30-fold for homologous and homeologous recombination, respectively. Based on our data and those of Myung et al. (2001), this high level of homeologous recombination is likely to contribute to the significant increase of Can^r mutations and GCRs observed in the *sgs1Δ* mutants during aging (Fig. 2 J).

Age-dependent mutations in *SGS1* deletion mutants originate both in nonquiescent and quiescent cells

The results presented indicate a significant age-dependent increase in mutation accumulation, GCRs, and recombinational events in the Sgs1-deficient strain when compared with the wild type. To understand whether the initial age-dependent DNA damage occurs in nondividing cells and to investigate the association between cell-cycle arrest and mutation frequency, we made use of the fractionation method recently described by Allen et al. (2006). The cultures subjected to the Percoll density gradient separated into two distinct fractions: the upper fraction, mainly composed of a heterogeneous population of nonquiescent cells that includes dividing, nondividing, apoptotic, and necrotic cells and the lower fraction of quiescent cells (Allen et al., 2006). The Can^r mutation frequency of both fractions derived from day-3, -5, and -7 cultures were measured.

In the DBY746 background, quiescent cells accounted for 40% of the wild-type population by day 3 (Fig. S4 A, available at http://www.jcb.org/cgi/content/full/jcb.200707154/DC1). This percentage gradually decreased to 13% by day 7. In contrast, on days 3 and 7, respectively, only 20 and 7% of the *sgs1Δ* cells were observed in the lower quiescent fraction (Fig. 3 A). Moreover, *sgs1Δ* cells displayed significantly higher percentages of budding indices (Fig. 3 B) over time in both fractions compared with wild type (Fig. S4 B), which suggests a defect in cell-cycle/G1 arrest and inability to enter into a true "quiescent" state. As expected, the deletion of *SGS1* caused a significant age-dependent increase of mutation frequency in both the upper and lower fractions when compared with the wild type (Fig. 3 C and Fig. S4 C). The mutation frequency levels detected in Sgs1-deficient cells were of the same order of magnitude before and after treatment with Percoll gradient, indicating that the cell separation procedure itself (including high Percoll concentrations) was not responsible for the increase of mutations.

To determine whether the initial DNA damage might form during cell division and not during aging, we allowed cells from days 1, 3, 5, and 7 of a standard CLS study to undergo one population doubling before treatment with the toxic canavanine. If the initial DNA damage did not occur during aging but during the reentry of aging cells into the cell cycle, we would expect the population doubling of all the 2×10^7 cells to cause a major increase in mutation frequency. Instead, we observed that the frequency of mutations normalized for population size remained the same for cells exposed to canavanine before or after one population doubling (Fig. 3 D), which suggests that at least the initial DNA damage in the *CAN1* gene occurs in nondividing cells during aging and becomes a mutation, deletion, or GCR during the first round of replication.

Deletion of oncogene homologue *SCH9*, but not severe calorie restriction (CR), blocks premature genomic instability in *sgs1Δ* mutants

We previously showed that yeast lacking *SCH9* or components of the Ras–PKA pathway are long-lived (Fabrizio et al., 2001, 2005; Longo, 2003). We, and others, have proposed that the down-regulation of the Sch9 and Ras–cAMP–PKA pathway delays aging and partially mediates the life-span extension caused by CR (Longo and Finch, 2003; Kaeberlein et al., 2005). CR is a well studied intervention that consistently extends the life span of organisms ranging from yeast to mice (Weindruch and and Walford, 1988; Weindruch, 1996; Lin et al., 2000; Fabrizio and Longo, 2003). Furthermore, recent results from our laboratory

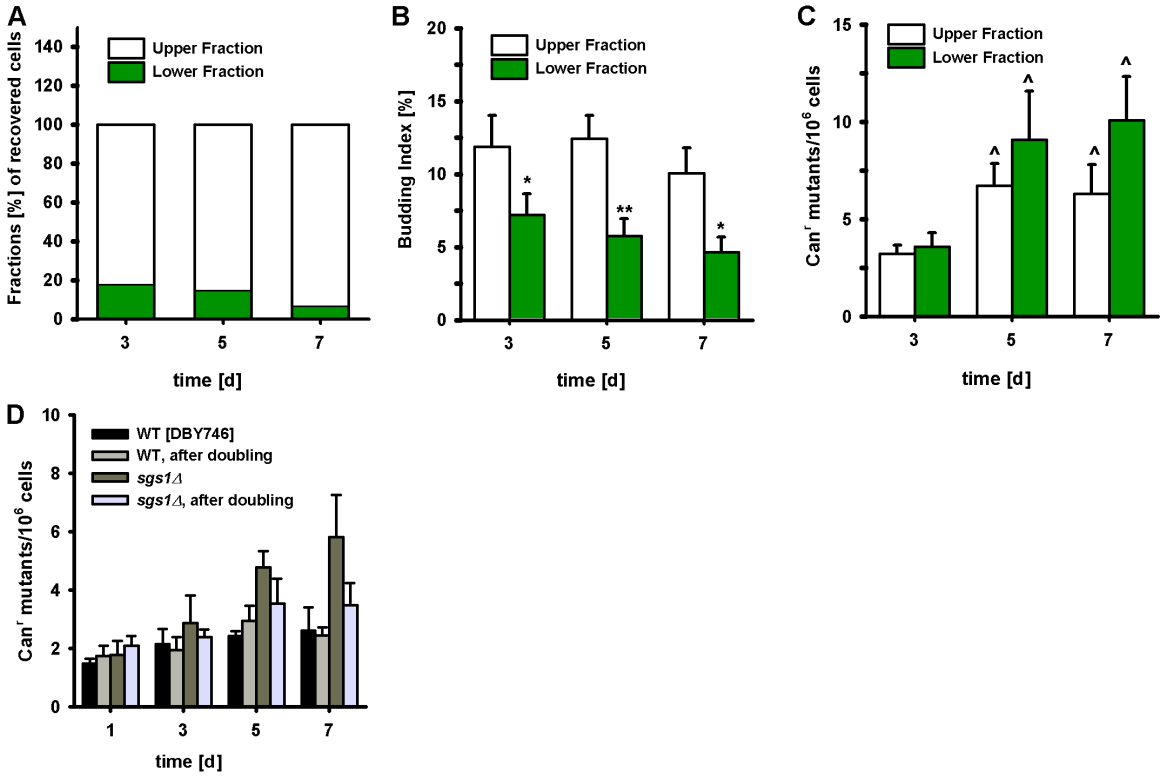

Figure 3. **Premature genomic instability in *sgs1Δ* mutants originates from both nonquiescent and quiescent cells.** (A) Fractions (%) of recovered cells from *sgs1Δ* chronological aging cultures subjected to a Percoll density-gradient separation. (B and C) Budding index (%; B) and *CAN1* mutation frequency (C) over time measured as Can^r mutants/10^6 cells are measured in upper and lower fractions. Data are shown as mean ± SEM (n = 4–5). *, $P < 0.05$; **, $P < 0.01$ (lower fraction vs. upper fraction). ^, $P < 0.05$ (vs. day 3). (D) *CAN1* mutation frequency over time measured as Can^r mutants/10^6 cells of wild-type and *sgs1Δ* mutant cells before and after doubling. On days 1, 3, 5, and 7 of a chronological aging study, cells were allowed to undergo one population doubling before plating on canavanine selective medium. The mean ± SEM is shown (n = 4).

showed that genomic instability was reduced at all ages in long-lived mutants lacking *SCH9* (Fabrizio et al., 2004, 2005). In the present study, we set out to determine whether the deletion of this oncogene homologue could also exert a protective effect against premature chronological age-dependent genomic instability in the *sgs1Δ*-null mutants.

Deletion of *SCH9* led to a significant CLS increase in *sgs1Δ* mutants, although the *sch9Δsgs1Δ* double mutant did not survive as long as the single *sch9Δ* mutant (Fig. 4 A and Fig. S3, B and C; Fabrizio et al., 2001, 2005). Notably, CR *sgs1Δ* mutants did not have a significantly longer mean life span compared with *sgs1Δ* mutants in glucose/ethanol medium, although they survived better at advanced ages (Fig. 4 B and Fig. S5, available at http://www.jcb.org/cgi/content/full/jcb.200707154/DC1).

Mutations in *SCH9*, but not CR, prevented the age-dependent Can^r mutations (Fig. 4, C and D) and GCRs (Fig. 4 E) caused by Sgs1 deficiency. In general, CR showed a positive protective trend, which was significant only at day 5. In agreement with the GCR frequency results, we were able to PCR amplify and sequence the entire *CAN1* gene in 80% of Can^r mutant colonies from a day-7 *sch9Δsgs1Δ* culture but only 50% of the *CAN1* genes obtained from *sgs1Δ* colonies (Table III). The most likely explanation is that GCRs caused a deletion of the region containing the primer sequence for the PCR amplification.

Notably, lack of *SCH9* actually increased *trp1-289* reversions in *sgs1Δ* mutants back to the wild-type level (Fig. 4 F), suggesting that the *sgs* deletion causes genomic instability but also prevents the activity of an error-prone repair system that causes C→T base substitutions, possibly by promoting recombination or death instead. Although C→T (G→A) base substitution was absent in *sgs1Δ*, it was present in *sch9Δsgs1Δ* (Table III). In contrast, lack of *SCH9* further decreased the small DNA insertions/deletions that cause Lys$^+$ reversions (Fig. 4 G), indicating that NHEJ repair may be reduced in these mutants.

To investigate the mechanisms responsible for the protective effect of lack of *SCH9* against *sgs1Δ* defects, we monitored age-dependent changes in cell-cycle profiles. The deletion of *SCH9* in *sgs1Δ* mutants increased the G1 arrest, as shown by the FACS analysis data, and caused a major reduction in budding index (Fig. 5, A and B; and Table II). Consistently, the frequency of chronological age-dependent dedifferentiation was reduced from 50% in *sgs1Δ* cultures to 12% in *sch9Δsgs1Δ* cultures (2 out of 21; $P = 0.036$ [Fisher's exact test]; Table I). Similarly, dedifferentiation was not observed in any of the *sch9Δsgs1Δ* cultures in the SP1 or BY4741 genetic backgrounds, although the number of samples was small (Table I). Thus, the deletion of *SCH9* reversed the dedifferentiation defects of *sgs1Δ* mutant cells by significantly reducing the budding index and tightening the G1 arrest (Fig. S4, A and B). Furthermore, it abolished the age-dependent increase in Can^r mutation frequency originated by both nonquiescent and quiescent *sgs1Δ* cells to levels similar to those of wild-type cells (Fig. S4 C).

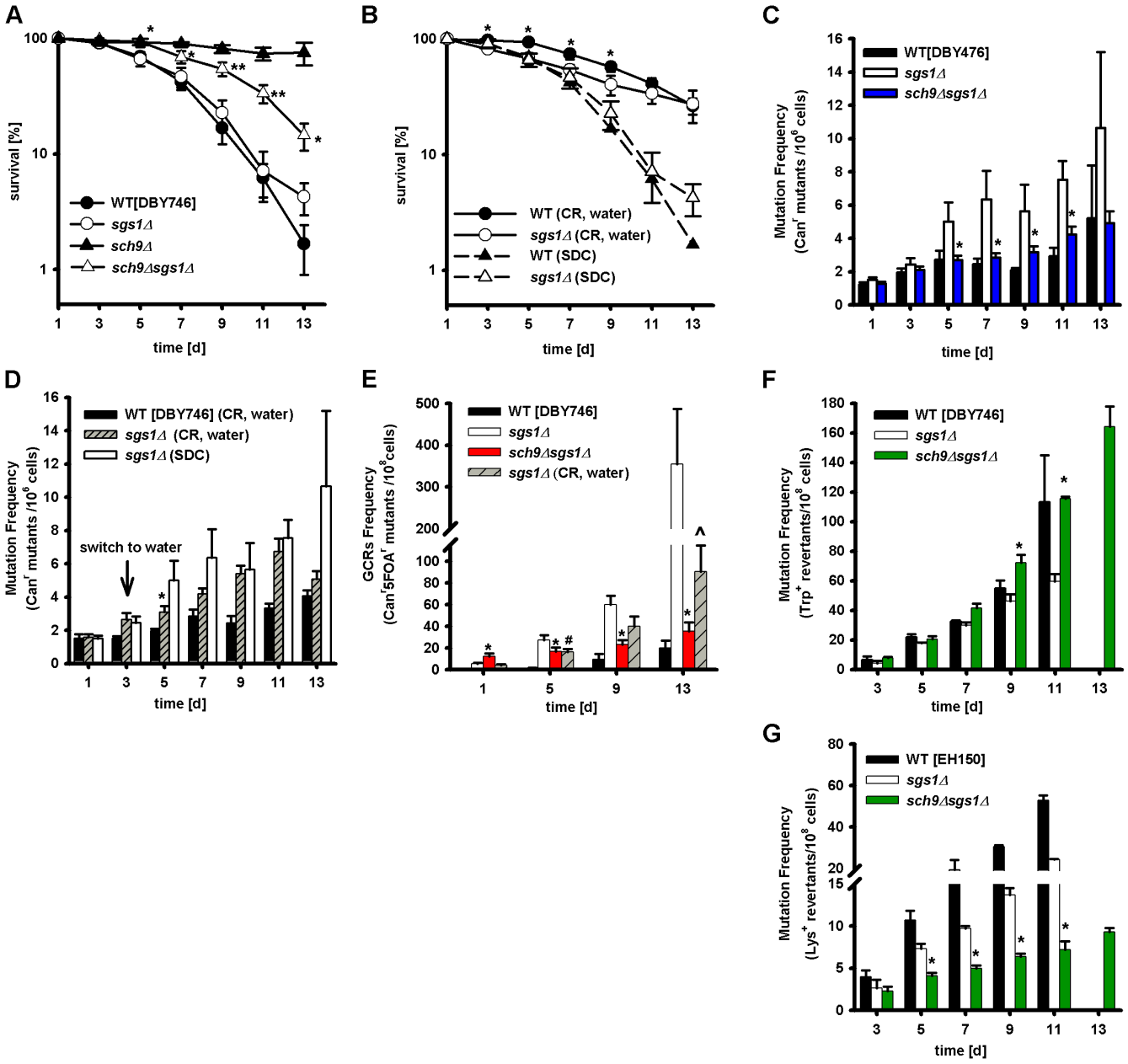

Figure 4. **Effect of deletion of oncogene homologue *SCH9* and starvation/severe CR on premature aging and genomic instability of *sgs1Δ* mutants.** (A) Survival of wild type and mutants lacking *SGS1*, *SCH9*, or both. The mean ± SEM is shown (n = 12–17). *, $P < 0.05$; **, $P < 0.01$ (*sch9Δsgs1Δ* vs. *sgs1Δ*). (B) Survival of wild-type strain and *sgs1Δ* mutant under starvation/CR. Data represent the mean ± SEM (n = 10–16). *, $P < 0.05$ (between calorie-restricted *sgs1Δ* and wild-type cells). (C) Age-dependent mutation frequency measured as Can^r mutants/10^6 cells of wild type and mutants lacking *SGS1* or both *SCH9* and *SGS1*. The mean ± SEM is shown (n = 12–17). *, $P < 0.05$ (*sch9Δsgs1Δ* vs. *sgs1Δ*). (D) Age-dependent mutation frequency measured as Can^r mutants/10^6 cells of calorie-restricted wild type and mutants lacking *SGS1*. Data represent the mean ± SEM (n = 10–16). *, $P < 0.05$ (calorie-restricted *sgs1Δ* vs. *sgs1Δ* in SDC). (E) GCR frequency measured as Can^{r}5FOA^r mutants/10^8 cells of wild type and mutants lacking *SGS1* or both *SCH9* and *SGS1* and calorie-restricted *sgs1Δ* mutant cells. Data represent the mean ± SEM (n = 7–11). *, $P < 0.05$; ^, $P < 0.05$ (*sch9Δsgs1Δ* vs. *sgs1Δ* in SDC or CR *sgs1Δ*, respectively); #, $P < 0.05$ (CR *sgs1Δ* vs. SDC *sgs1Δ*). (F and G) Effect of the *SCH9* deletion on the age-dependent *trp1-289* reversion frequency (F) and the rate of small insertion/deletion mutations in the *lysΔBgl* strain (EH150) of *sgs1Δ* mutants (G). The means ± SEM are shown (n = 7–14). *, $P < 0.05$ (*sch9Δsgs1Δ* vs. *sgs1Δ*).

In the previous section, we showed that the deletion of *SGS1* caused a major increase in homologous and homeologous recombination during chronological aging. To determine whether the protective effect of *sch9Δ* might be caused by attenuating recombination, we monitored age-dependent homologous and homeologous recombination frequency. Both homologous and homeologous recombination were greatly reduced in *sch9Δsgs1Δ* compared with *sgs1Δ* cells (Fig. 5, C and D). Together with the previous studies by Kolodner and co-workers, our results suggest that the lack of *SCH9* prevents the age-dependent genomic instability defects in *sgs1Δ* mutants in part through inhibition of erroneous recombination between sister chromatids (Myung et al., 2001; Myung and Kolodner, 2002).

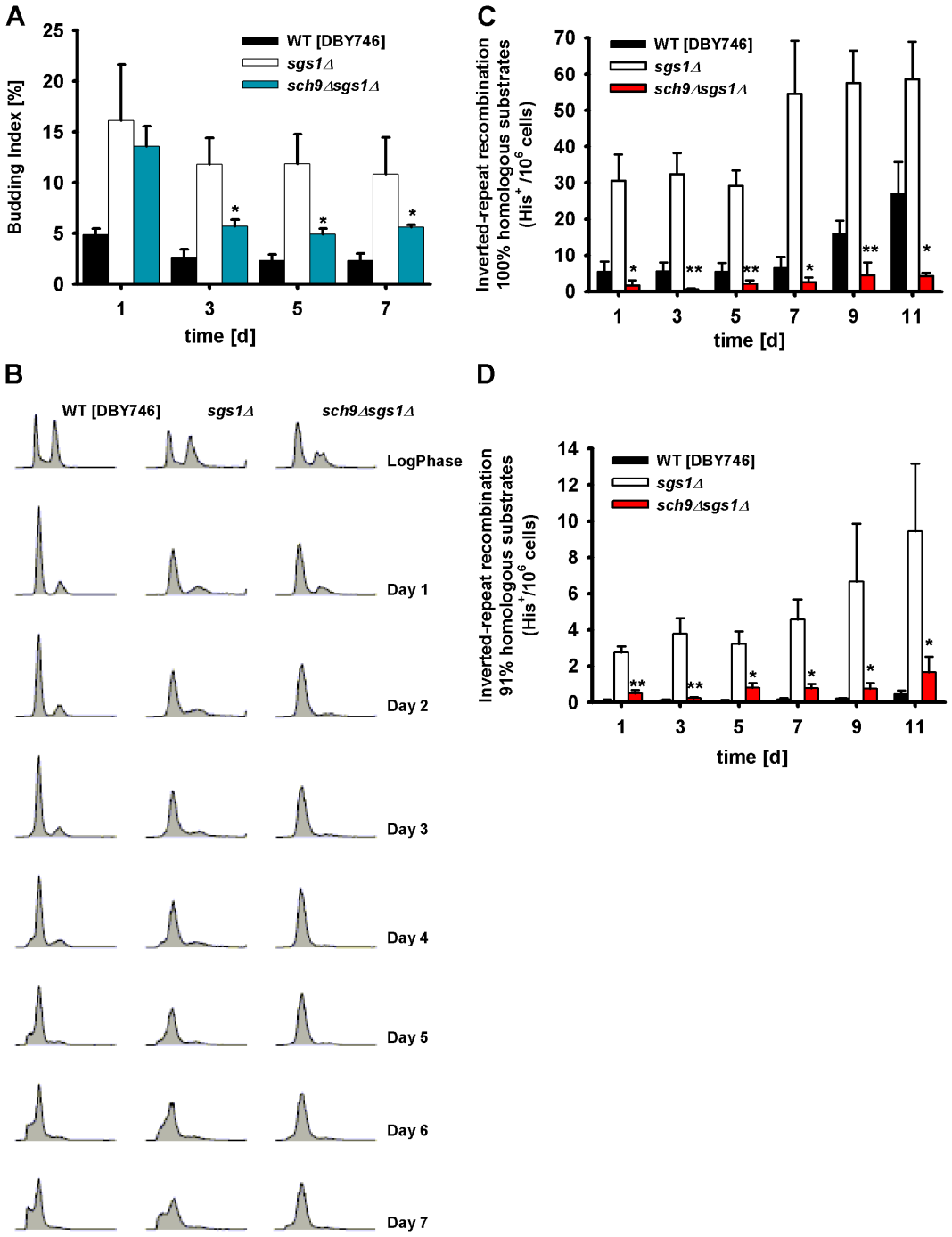

Figure 5. **Effect of lack of *SCH9* on the cell-cycle profiles and recombinational events of *sgs1Δ* mutants.** (A) Age-dependent variation of the percentage of budded cells measured as described in Materials and methods. Data represent the mean ± SEM (n = 3). (B) Representative cell-cycle profile (FACS) of wild type and mutants lacking *SGS1* or both *SCH9* and *SGS1*. (C and D) Homologous (C) and homeologous (D) recombination frequency measured as His^+ colonies/10^6 cells during chronological aging of wild-type, *sgs1Δ*, and *sch9Δsgs1Δ* mutants. The mean ± SEM is shown (n = 4). *, $P < 0.05$; **, $P < 0.01$ (*sch9Δsgs1Δ* vs. *sgs1Δ*).

To determine whether the lack of Sch9 might protect against genomic instability in *sgs1Δ* mutants by either protecting against the initial damage of DNA or enhancing DNA repair, we monitored the changes in Can^r mutations and GCR frequencies upon treatment of oxidant (100 mM hydrogen peroxide) or alkylating agent (0.02% MMS). After treatment, 3-d-old cells were washed four times and allowed to recover in a toxin-free medium for up to 5 h. Can^r mutations and GCRs were measured 30 min and 2 and 5 h after treatment. The lack of Sch9 activity protected *sgs1Δ* against oxidation-dependent viability loss as well as Can^r mutations and GCRs (Fig. 6, A–C). The deletion of *SCH9* also partially reversed the hypersensitivity of *sgs1Δ* to chronic treatment with H_2O_2 (Fig. 7, A and B).

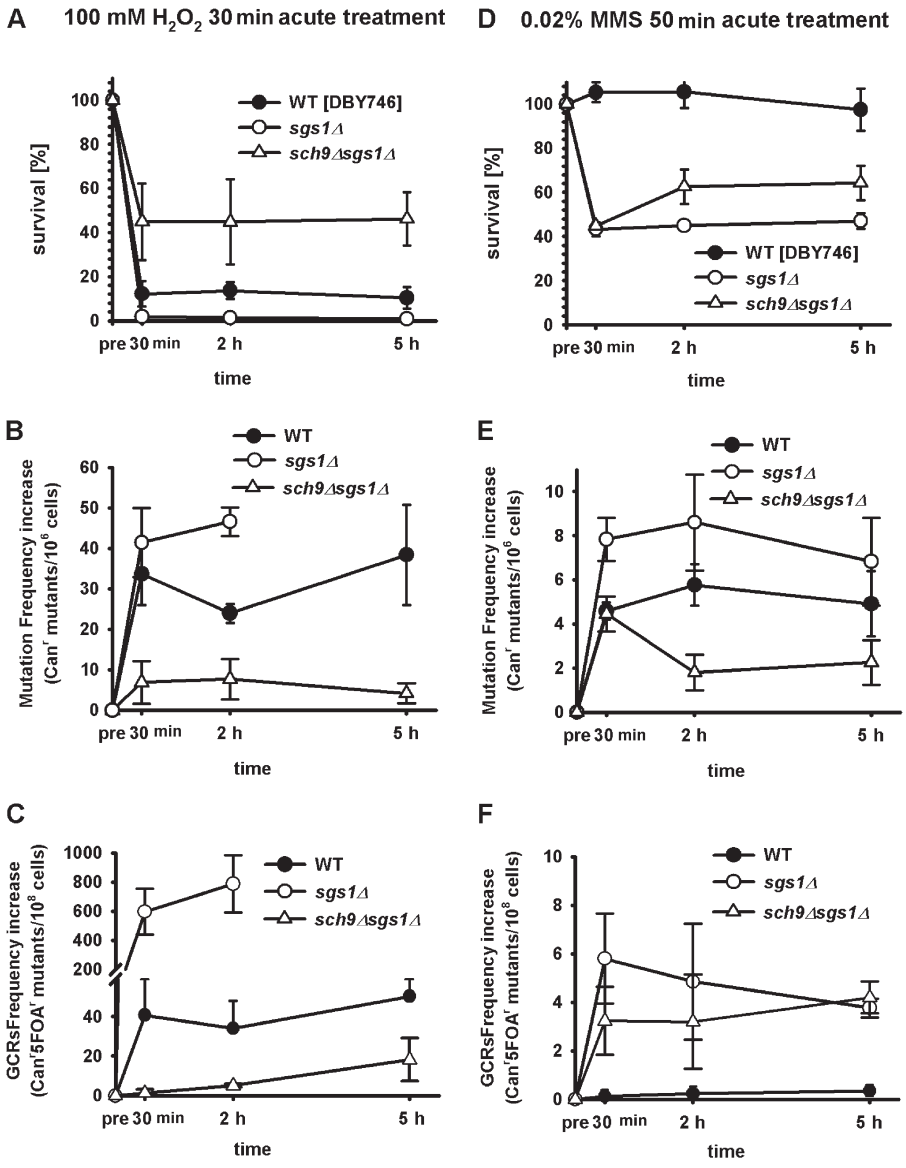

Figure 6. **Effect of lack of *SCH9* on the time-dependent repair of oxidation or alkylation-induced mutations in *sgs1Δ* mutants.** (A–C) Survival of wild-type (DBY746), *sgs1Δ*, or *sch9Δsgs1Δ* mutants after 30 min of exposure to 100 mM H_2O_2 (A). After treatment, cells were centrifuged, washed four times, and re-suspended in H_2O_2-free medium obtained from day-3 wild-type culture. Mutation frequency, measured as Can^r mutants/10^6 cells (B) and GCRs (Can^{r}5FOA^r mutants/10^8cells; C), was monitored at the indicated times (30 min and 2 and 5 h). (D) Survival of wild-type, *sgs1Δ*, or *sch9Δsgs1Δ* mutants after exposure to 0.02% MMS for 50 min. After treatment, cells were centrifuged, washed four times, and re-suspended in MMS-free medium obtained from day-3 wild-type culture. Mutation frequency, measured as Can^r mutants/10^6 cells (E) and GCRs (F; Can^{r}5FOA^r mutants/10^8cells), was monitored at the indicated times (30 min and 2 and 5 h). In both experiments, ~30 min was the minimum required time from the end of treatment to centrifuge, wash, and resuspend the cells before plating. The mean ± SEM is shown (n = 3).

Although the majority of *sgs1Δ* cells died after 2-h treatment with hydrogen peroxide, the survivors showed a 20-fold increase of Can^r mutation frequency and a 65-fold increase in GCR frequency (Fig. 6, B and C). To exclude the possibility that this increase in DNA damage in both wild-type and *sgs1Δ* cells was not representative of the damage caused by oxidative treatment but rather a characteristic of very sick cells, both strains were exposed to a reduced dose of hydrogen peroxide (50 mM). The lower dose of hydrogen peroxide had a smaller effect on cell death but caused DNA damage comparable to that at the higher dose (unpublished data).

In contrast to the results with oxidative stress, cells lacking *SGS1* died after treatment with MMS, even in combination with *sch9Δ* mutations (Fig. 6 D). Although the lack of *SCH9* protected against MMS-induced Can^r mutations, it did not protect against GCRs (Fig. 6, D and F). These results indicate that the *SCH9* deletion protects against DNA damage in *sgs1Δ* mutants in part by preventing the initial oxidation-dependent DNA damage, which is in agreement with our previous results indicating that superoxide is a major contributor to age-dependent mutations (Fabrizio et al., 2003, 2004).

Discussion

Mutations in the human WRN and BLM RecQ helicases cause accelerated aging (WS) and premature age-dependent cancer (BS), respectively. Because *S. cerevisiae* is known to express only one RecQ helicase, the combination of the deletion of the *SGS1* gene and CLS analysis provides a simple system to study the fundamental role of RecQ helicases in age-dependent genomic instability. Whereas Sgs1-deficient strains either had a normal or slightly decreased CLS when maintained in standard glucose/ethanol medium, they showed increased mortality under starvation/extreme CR (Fig. 4 B, water) or when treated with hydrogen peroxide or the mutagen MMS (Fig. 1, A and B). *sgs1Δ* mutants showed early dedifferentiation and regrowth phenotype associated with G1 arrest deficiencies and a three- to fourfold increase of budding index (Fig. 1, E and F; and Table I)

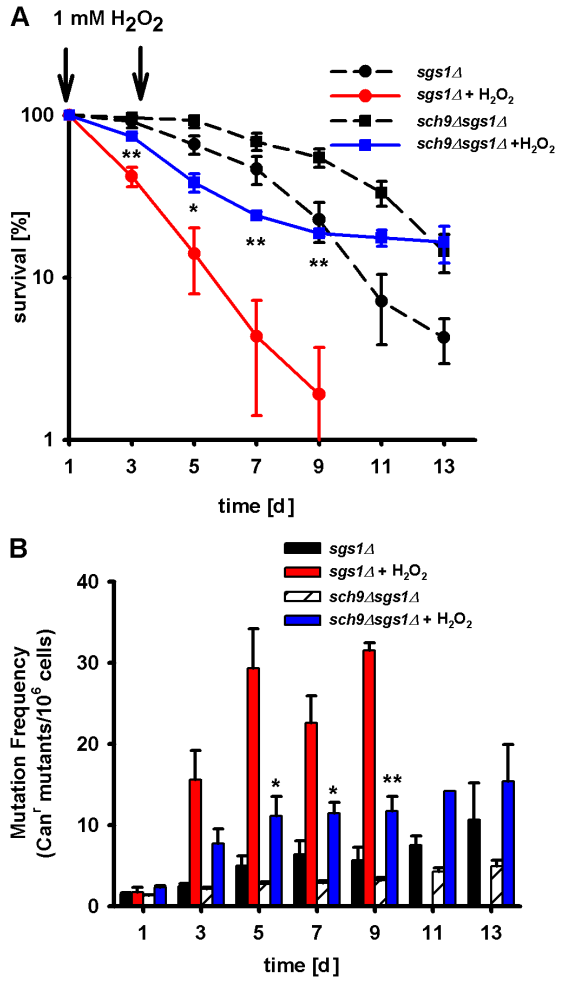

Figure 7. **Protective effect of lack of *SCH9* against oxidative stress in *sgs1Δ* mutants.** (A and B) Chronological survival (A) and mutation frequency (B) over time in the *CAN1* gene, measured as Can^r mutants/10^6 cells of *sgs1Δ* and *sch9Δsgs1Δ* cells, either untreated or chronically (days 1 and 3) exposed to 1 mM H_2O_2. Data represent the mean ± SEM (n = 4). *, P < 0.05; **, P < 0.01 (*sch9Δsgs1Δ*-treated vs. *sgs1Δ*-treated cells).

reminiscent of the early cancer phenotype of BS. This early/increased dedifferentiation phenotype was observed in three different genetic backgrounds.

In agreement with the studies performed in dividing *S. cerevisiae* (Myung et al., 2001), young (day 1) Sgs1-deficient cultures displayed a frequency of *CAN1* mutations similar to that of wild type in two different genetic backgrounds (DBY746 and BY4741). However, a higher increase in age-dependent *CAN1* mutation frequency and GCR formation occurred in *sgs1Δ* mutants compared with wild-type cells (Fig. 2, A and B). Notably, specific base substitutions (C→T) and small DNA insertion/deletion mutations were actually reduced in aging *sgs1Δ* mutants, which raises the possibility that the higher rate of recombination between sister chromatids performed in these mutants replaces other types of error-prone repair systems that cause base substitutions or small insertions/deletions. Interestingly, the loss of multiple Sgs1-dependent functions might be at the base of part of the age-dependent DNA damage in *sgs1Δ* cells because cells lacking only the helicase domain, the C-terminal checkpoint domain, or the Top3-binding domain of Sgs1 did not show similar levels of Can^r mutations when compared with cells lacking the entire protein (*sgs1Δ*). An alternative explanation is that additional domains that are important for genomic stability remain to be identified. In contrast, the lack of the DNA helicase domain of Sgs1 was sufficient to cause a major age-dependent increase in the formation of GCRs, whereas at advanced ages this increase was lower than that caused by the deletion of the entire *SGS1* gene (Fig. 2 G, *sgs1Δ*).

It is remarkable that the age-dependent frequency of GCRs that occurred in nondividing cells reached a level that was 40-fold higher than that obtained after many cycles of cell divisions required to reach a population density of $\sim 100 \times 10^6$ cells on day 1. This underscores the importance of performing age-dependent studies in addition to studies in the growth phase.

The following results suggest that reduced recombination is a key component of the protective effect of the lack of *SCH9* against the premature aging phenotypes caused by the deletion of *SGS1*: The protection against age-dependent Can^r mutations and GCR, but not trp, reversions (Fig. 4, C, E, and F); the reversion in *sch9Δsgs1Δ* of the major increase in the rate of homologous and homeologous recombination caused by the deletion of *SGS1* (Fig. 5, C and D); the attenuation of GCRs confirmed by the frequency results and the sequencing data (a lack of major portions of the *CAN1* gene observed in only 20% of *sch9Δsgs1Δ* but 50% of *sgs1Δ*; Fig. 4 E and Table III); and previous studies conclude that homeologous recombination plays a central role in GCRs in growing *sgs1Δ* cells (Myung et al., 2001).

The other major protective effect caused by the deletion of *SCH9* appears to be the prevention of the initial DNA damage. In fact, *sch9Δsgs1Δ* cells were protected against both acute and chronic treatment with hydrogen peroxide (Figs. 6 and 7). The acute oxidative stress experiments suggest that *sch9Δ* is blocking the initial DNA damage or mutations rather than increasing the rate of repair. This protection is likely to involve antioxidant enzymes as well as additional protective systems (Longo et al., 1996, 1999; Fabrizio et al., 2003).

The G1-arrest defects of *sgs1Δ* could explain the sixfold increase in the percentage of age-dependent dedifferentiation (Fig. 1 and Table I). These defects, which may derive from the lack of the cell-cycle arrest C200 domain of Sgs1, are reversed by the deletion of *SCH9* (Fig. 5 and Table I). In contrast, the finding that the frequency of age-dependent mutations is higher in the quiescent fraction of *sgs1Δ* cells compared with the nonquiescent fraction suggests that the cell-cycle defects are not a major promoter of mutation (Fig. 3). One possibility is that a major portion of the *sgs1Δ* cells that have DNA damage but fail to arrest, die, possibly because of double-strand breaks. Starvation/extreme CR showed a promising protective trend but not a significant effect against genomic instability during most of the CLS of *sgs1Δ* mutants. Although further experiments in yeast and other model systems should be performed to test further the role of CR against age-dependent DNA damage, these results are consistent with our previous conclusion that even extreme CR is not as effective as mutations in *SCH9* in protecting against age-dependent damage and aging (Fig. 4 and Fig. S5; Longo, 1997; Longo et al., 1997; Fabrizio et al., 2005).

We previously showed that superoxide plays a primary role in chronological age-dependent DNA damage and mutations. Our model is that the DNA damage caused by oxidative and other types of stress accumulated during aging in nondividing cells generates double-strand breaks during the first round of replication after the exit from G_0. Cells lacking *SGS1* attempt to repair this damage by homologous recombination between sister chromatids but generate a large number of GCRs, especially at advanced age.

This study raises the possibility that down-regulation of Akt/mTOR/S6kinase or upstream proteins implicated in life-span regulation may protect against age-dependent DNA damage and cancer, including the premature defects observed in WS and BS (Hasty and Vijg, 2002). Naturally, the connection between oncogenes or protooncogenes and age-dependent genomic instability demonstrated in the *S. cerevisiae* model must first be established in higher eukaryotes. However, our findings are consistent with the recent observation that in the *Ercc1*$^{-/-}$ mouse, a model of the human XPF progeroid syndrome, the growth hormone/IGF1 hormonal axis is suppressed in response to cytotoxic DNA damage (Niedernhofer et al., 2006; Vijg and Suh, 2006), which raises the possibility that reduced IGF-I–Akt–mTOR–S6kinase signaling might protect against the accelerated rate of DNA damage in this model. Furthermore, these mice showed similar patterns of metabolic and growth changes to those already observed under CR conditions (Spindler, 2005). Thus, it will be important to determine whether the down-regulation of the IGF-I–Akt–mTOR–S6kinase pathway may have a similar effect in protection of mouse model systems for WS and BS.

Materials and methods

Yeast strains and growth conditions

The majority of the experiments were performed in DBY746 (*MATα,leu2-3, 112,his3Δ1,trp1-289,ura3-52,GAL*$^+$; provided by D. Botstein, Massachusetts Institute of Technology, Cambridge, MA). Strains BY4741 (*MATa,his3Δ1leu2Δ0,met15Δ0,ura3Δ0*; Open Biosystems) and SP1 (*MATα, his,leu2,ura3,trp1,ade8 can1*; provided by J. Valentine, University of California, Los Angeles, Los Angeles, CA) were used to confirm the results obtained with DBY746. Strain EH150 *(MATa,lys2ΔBglII,trp1-Δ,his3-Δ200,ura3-52,ade2-1o*) was used for the small insertion/deletion mutation assay (provided by E. Heidenreich, Institute of Cancer Research, Medical University of Vienna, Vienna, Austria).The *sch9Δ* mutant has been described previously (Fabrizio et al., 2001).

All the mutant strains were originated in the different backgrounds by one-step gene replacement according to Brachmann et al. (1998). To generate the *sgs1* mutated derivatives, we used the following plasmids: pJM526 (*SGS1*), pJM511 (*sgs1-hd*), pJM531 (*sgs1-DN50*), and pJM512 (*sgs1-DC200*; provided by B. Johnson, University of Pennsylvania School of Medicine, Philadelphia, PA; Mullen et al., 2000). Each plasmid was digested with BStEII and transformed in DBY746. Proper integration of a single copy of each *sgs1* mutant at the *LEU2* locus was confirmed by PCR. Strains for intron-based inverted-repeat recombination assay were constructed using plasmids provided by S. Jinks-Robertson (Emory University, Atlanta, GA; Datta et al., 1996). Plasmids pRS406 (carrying two 100% homologous inverted repeats [IRs]) and pRS407 (carrying two 91% homologous IRs) were linearized with StuI before transformation. *Ura*$^+$ transformants with a single copy of integrated HIS3::intron-IR cassette derived from wild-type (DBY746), *sgs1*Δ, or *sch9*Δ *sgs1*Δ strains were used for recombination assay. CLS of cells incubated in either minimal medium containing glucose (synthetic dextrose complete [SDC]) or water was measured as described previously (Fabrizio and Longo, 2003). In brief, yeast were grown in synthetic medium (SDC) containing 2% glucose and supplemented with amino acids, adenine, and uracil (as previously described in Kaiser et al. [1994]), as well as a fourfold excess of the supplements tryptophan, leucine, uracil, and histidine. CLS was monitored in expired SDC medium by measuring colony-forming units (CFUs) every 48 h. The number of CFUs on day 1 was considered as the initial survival (100%) and was used to determine the age-dependent mortality. CLS was also monitored by counting yeast cells stained with 0.01 mg/ml phloxin B using a standard hemocytometer chamber (Kucsera et al., 2000). For life-span experiments in water (CR), yeast were grown in SDC for 3 d, washed with sterile distilled water, and resuspended in water. Yeast cells were washed with water every 48 h to avoid the accumulation of nutrient release from dead cells.

Stress-resistance assays

Heat-shock resistance was measured by spotting serial dilutions of cells removed from day-3 postdiauxic-phase cultures onto yeast extract peptone dextrose medium (YPD) plates and incubating at 55 (heat shocked) and 30°C (control) for 90 min. After heat shock, plates were transferred at 30°C and incubated for 2–3 d.

For oxidative stress–resistance assays, acute treatment exponentially growing (OD_{600} = 1) or day-3 postdiauxic-phase cells were diluted to an OD_{600} of 0.1 in potassium phosphate buffer, pH 7.4, and treated with 250 μM menadione for 60 min. Serial dilutions of untreated and menadione-treated cells were spotted onto YPD plates and incubated at 30°C for 2–3 d. Alternatively, cells were diluted to an OD of 1 in potassium phosphate buffer, pH 6, and treated with 100 mM hydrogen peroxide for 30 min.

SDC liquid medium cell cultures were also chronically treated with either 1 mM hydrogen peroxide or 0.001% MMS on days 1 and 3 of a typical chronological aging study.

Mutation-frequency measurements

Spontaneous mutation frequency was evaluated by measuring the frequency of mutations of the *CAN1* (*YEL063*) gene. In brief, overnight inoculations were diluted in liquid SDC medium and incubated at 30°C. Cell viability was measured every 2 d starting at day 1 by plating appropriate dilutions onto YPD plates and counting the CFUs. To identify the canavanine-resistant mutants (Can^r) in the liquid culture, an appropriate number of cells (starting amount, 2×10^7 cells) was harvested by centrifugation, washed once with sterile water, and plated on selective medium (SDC-ARG supplemented with 60 μg/ml L-canavanine sulfate). Mutant colonies were counted after 3–4 d. The mutation frequency was expressed as the ratio of Can^r over total viable cells.

The Can^r mutator phenotype can be conferred by any mutations that block the expression of the *CAN1* gene (Chen and Kolodner, 1999). Thus, we measured base substitutions, small insertions/deletions, or GCRs to specifically characterize the age-dependent type of mutations occurring in wild-type and mutant strains (Madia et al., 2007).

Large-scale measurement of GCRs

To detect GCRs, we generated a DBY476 background strain in which we replaced *HXT13* (*YEL069*), encoding for a highly redundant hexose transporter, with a *URA3* cassette as described by Chen and Kolodner (1999). *HXT13* is located 7.5 kb telomeric to *CAN1* on chromosome V. The experiment was conducted similarly to that described for the *can1* mutations but the detection for the loss of both *CAN1* and *URA3* was performed on SDC-ARG plates containing 1 mg/ml 5-fluoroorotic acid (5FOA) and 60 μg/ml L-canavanine. Mutant colonies were counted after 3–4 d.

Measurement of age-dependent small insertion/deletion mutations

Based on the experimental design proposed by Heidenreich et al. (2003) and Heidenreich and Wintersberger (1998), we generated *sgs1Δ* and *sch9Δsgs1Δ* mutants in a Lys$^-$ strain (EH150) in which a lys2ΔBglII mutation was constructed by filling in a BglII restriction site of the *LYS2* gene. The resulting +4 shift in the ORF causes an auxotrophy for lysine that can be reversed by small age-dependent insertion/deletion mutations. Using these strains, we have monitored the age-dependent insertion/deletion events after plating 10^8 cells on selective SDC-LYS plates. The experiments were performed similarly to that described for the *can1* mutations.

Measurement of age-dependent single-base substitution mutations.

To monitor the frequency of reversion of a base substitution, we used the strain DBY746, which carries a *trp1-289* amber mutation (C→T at residue 403 of the coding sequence), and measured the frequency of *trp1-289* to Trp$^+$ reversions (Capizzi and Jameson, 1973). The experimental protocol was similar to the one described for the small insertion/deletion mutations detection. 10^8 cells were plated onto selective medium (SDC-TRP). The experiments were performed similarly to that described for the *can1* mutations.

Recombination assay

To monitor the level of homologous (100%) and homeologous (91%) recombination during chronological aging, we generated mutants in which

we integrated linearized plasmids carrying either 100% homologous IRs (pRS406) or 91% homeologous IRs (pRS407; Datta et al., 1996). *Ura*$^+$ transformants with a single copy of integrated HIS3::intron-IR cassette derived from wild-type (DBY746), *sgs1*Δ, or *sch9*Δ *sgs1*Δ strains were used. Starting from day 1 of a standard chronological aging study, homologous or homeologous His$^+$ recombinants were measured by plating 5×10^7 viable cells (washed twice with sterile water) every 2 d on selective medium (synthetic complete medium lacking HIS and supplemented with galactose according to Datta et al. [1996]). The number of *His*$^+$ colonies was counted 4 d after plating, and the frequency of homologous or homeologous recombination was calculated based on the number of viable cells.

FACS analysis and budding index

Cells from exponentially proliferating cultures of wild-type, *sgs1*Δ, and *sch9*Δ*sgs1*Δ strains were inoculated into SDC medium at an initial density of 5×10^5/ml and continuously cultured for 7 d at 30°C with rotary shaking. Aliquots of cells removed from each culture at the indicated times were pelleted by centrifugation and resuspended in water (for determining the fraction of budding cells) or 70% ethanol. To measure budding index, cells were sonicated using a Sonic Dismembrator sonicator (model 60; Thermo Fisher Scientific) for 10 s at power setting 5. The fraction of budding cells (budding index) of at least 500 cells from each aliquot was visually determined using a microscope (E600 Eclipse; Nikon) with a 40× phase-contrast objective. To measure DNA content by flow cytometry, cells suspended in 70% ethanol were pelleted by centrifugation, washed with 50 mM sodium citrate, pH 7.5, and resuspended in 0.5 ml of this same buffer containing 0.5 mg/ml RNase (Invitrogen). After overnight incubation at 37°C, 0.5 ml sodium citrate buffer containing 2 μM SYTOX green (Invitrogen) was added to each sample. Stained cells were briefly sonicated as described in this section, and DNA content was measured using a FacsCaliber flow cytometer (BD Biosciences) at a maximum flow rate of 500 cells per second. Flow cytometry data were processed using CellQuest (BD Biosciences) and Flojo (Tree Star, Inc.) software. Data were calculated using MODFIT (Verity Software House). Data from FACS measurements presented in Figs. 1 E and 5 B are reported in Table II.

Separation of cells through a Percoll density gradient

A Percoll density gradient (GE Healthcare) was prepared using the protocol described by Allen et al. (2006). In brief, $\sim 2 \times 10^9$ cells from *sgs1*Δ and *sch9*Δ*sgs1*Δ SDC cultures were collected at days 3, 5, and 7 of a chronological aging study. Cells were pelleted and resuspended in 1 ml Tris buffer, overlaid on the preformed Percoll gradient, and centrifuged at 400 g_{av} for 60 min at 20°C. Fractions were collected, washed once with 40 ml Tris buffer, pelleted, and resuspended in ddH_2O. Immediately after the separation, cells were plated on YPD and on SDC-ARG supplemented with 60 μg/ml L-canavanine sulfate solid media to measure viability (CFUs) and determine mutation frequency, respectively. Three independent experiments were performed.

Lower and upper fraction cells were examined microscopically, without previous sonication, for the presence of new buds. Five fields of 50–60 cells were examined per time point and the budding percentage was calculated by comparing the number of cells with new buds to the total number of cells counted.

***CAN1* sequencing**

Canavanine-resistant clones from wild-type, *sgs1*Δ, and *sch9*Δ*sgs1*Δ strains were collected on day 7 of a CLS study. Genomic DNA was isolated using standard glass beads/chloroform-phenol procedure. The two primer sets used for PCR amplification to cover the *CAN1* open reading frame were the following: v-534 (5′-GAAGAGTGGTTGCGAACAGAG-3′) and v-555 (5′-CCTAAGAACCTCCCTTCGTTTT-3′) to amplify a 1080-bp region (−226 to approximately +854); and v-557 (5′-ATCACTTTTGCCCTGGAACTTA-3′) and v-270 (5′-CGTGGAAATGTGATCAAAGGTA-3′) to amplify a 1275-bp region (+535 to approximately +1809). 30 ng/ml of genomic DNA in a 50-μl reaction was subject to 30–35 cycles of amplification (94°C, 30 s; 52°C, 45 s, 72°C, 2 min 15 s). PCR products were gel purified and sequenced using the amplification primers (both directions). The additional primers used to confirm the sequencing results when necessary were the following: v-279 (5′-CTTAACTCCTGTAAAAAC-3′), v-280 (5′-TATTGGTATGATTGCCCTTG-3′), v-281 (5′-GAGTTCTGGGTCGCTTCCATC-3′), v-282 (5′-CAATCTACTTCCTACGTTTC-3′), and v-283 (5′-CGGTAACCCCAGCACCAC-3′). All primers were synthesized by Integrated DNA Technologies, Inc. Sequencing was performed by Laragen, Inc. Identification of mutation was performed using Mutation Surveyor v3.00 (Softgenetics).

Statistical analysis

Longevity curves and mutation-frequency curves were analyzed by either *t* test ($P < 0.001$, $P < 0.01$, and $P < 0.05$) or Mann-Whitney test on the data for each pair of strains at each day of the chronological aging study. Fisher's exact test was used to compare the percentage of dedifferentiation between wild-type, *sgs1*Δ, and *sch9*Δ*sgs1*Δ mutant cultures.

Online supplemental material

Fig. S1 shows chronological survival of *sgs1*Δ in BY4741 and SP1 backgrounds. Fig. S2 shows the methods of monitoring age-dependent mutation frequency using CLS. Fig. S3 shows premature genomic instability in the *sgs1*Δ mutant in the BY4741 background and the effect of lack of *SCH9* on premature aging in the *sgs1*Δ mutant in the BY4741 and SP1 backgrounds. Fig. S4 shows the separation of quiescent and nonquiescent cells, through a Percoll density gradient, from chronologically aging wild-type and *sch9*Δ*sgs1*Δ cultures. Fig. S5 shows the effect of lack of *SCH9* and CR on survival and mutation frequency of the *sgs1*Δ mutant. Online supplemental material is available at http://www.jcb.org/cgi/content/full/jcb.200707154/DC1.

We thank Dr. Sue Jinks-Robertson for providing us plasmids pRS406 and pS407 and Dr. E. Heindereich for providing strain EH150. We thank Myron Goodman and Michael Lieber for very helpful comments.

This work was supported in part by an American Federation for Aging Research grant and by National Institutes of Health grants AG20642, AG025135, and GM075308.

Submitted: 24 July 2007
Accepted: 12 December 2007

References

Allen, C., S. Buttner, A.D. Aragon, J.A. Thomas, O. Meirelles, J.E. Jaetao, D. Benn, S.W. Ruby, M. Veenhuis, F. Madeo, and M. Werner-Washburne. 2006. Isolation of quiescent and nonquiescent cells from yeast stationary-phase cultures. *J. Cell Biol.* 174:89–100.

Azam, M., J.Y. Lee, V. Abraham, R. Chanoux, K.A. Schoenly, and F.B. Johnson. 2006. Evidence that the *S. cerevisiae* Sgs1 protein facilitates recombinational repair of telomeres during senescence. *Nucleic Acids Res.* 34:506–516.

Bennett, R.J., and J.C. Wang. 2001. Association of yeast DNA topoisomerase III and Sgs1 DNA helicase: studies of fusion proteins. *Proc. Natl. Acad. Sci. USA.* 98:11108–11113.

Bennett, R.J., and J.L. Keck. 2004. Structure and function of RecQ DNA helicases. *Crit. Rev. Biochem. Mol. Biol.* 39:79–97.

Boulton, S.J., and S.P. Jackson. 1996. *Saccharomyces cerevisiae* Ku70 potentiates illegitimate DNA double-strand break repair and serves as a barrier to error-prone DNA repair pathways. *EMBO J.* 15:5093–5103.

Brachmann, C.B., A. Davies, G.J. Cost, E. Caputo, J. Li, P. Hieter, and J.D. Boeke. 1998. Designer deletion strains derived from *Saccharomyces cerevisiae* S288C: a useful set of strains and plasmids for PCR-mediated gene disruption and other applications. *Yeast.* 14:115–132.

Capizzi, R.L., and J.W. Jameson. 1973. A table for the estimation of the spontaneous mutation rate of cells in culture. *Mutat. Res.* 17:147–148.

Chen, C., and R.D. Kolodner. 1999. Gross chromosomal rearrangements in *Saccharomyces cerevisiae* replication and recombination defective mutants. *Nat. Genet.* 23:81–85.

Chen, C., K. Umezu, and R.D. Kolodner. 1998. Chromosomal rearrangements occur in *S. cerevisiae* rfa1 mutator mutants due to mutagenic lesions processed by double-strand-break repair. *Mol. Cell.* 2:9–22.

Cobb, J.A., and L. Bjergbaek. 2006. RecQ helicases: lessons from model organisms. *Nucleic Acids Res.* 34:4106–4114.

Datta, A., A. Adjiri, L. New, G.F. Crouse, and S. Jinks Robertson. 1996. Mitotic crossovers between diverged sequences are regulated by mismatch repair proteins in *Saccaromyces cerevisiae*. *Mol. Cell. Biol.* 16:1085–1093.

Ellis, N.A., J. Groden, T.Z. Ye, J. Straughen, D.J. Lennon, S. Ciocci, M. Proytcheva, and J. German. 1995. The Bloom's syndrome gene product is homologous to RecQ helicases. *Cell.* 83:655–666.

Epstein, C.J., G.M. Martin, A.L. Schultz, and A.G. Motulsky. 1966. Werner's syndrome a review of its symptomatology, natural history, pathologic features, genetics and relationship to the natural aging process. *Medicine (Baltimore).* 45:177–221.

Fabre, F., A. Chan, W.D. Heyer, and S. Gangloff. 2002. Alternate pathways involving Sgs1/Top3, Mus81/ Mms4, and Srs2 prevent formation of toxic recombination intermediates from single-stranded gaps created by DNA replication. *Proc. Natl. Acad. Sci. USA.* 99:16887–16892.

Fabrizio, P., and V.D. Longo. 2003. The chronological life span of *Saccharomyces cerevisiae*. *Aging Cell.* 2:73–81.

Fabrizio, P., F. Pozza, S.D. Pletcher, C.M. Gendron, and V.D. Longo. 2001. Regulation of longevity and stress resistance by Sch9 in yeast. *Science.* 292:288–290.

Fabrizio, P., L.L. Liou, V.N. Moy, A. Diaspro, J.S. Valentine, E.B. Gralla, and V.D. Longo. 2003. SOD2 Functions downstream of Sch9 to extend longevity in yeast. *Genetics.* 163:35–46.

Fabrizio, P., L. Battistella, R. Vardavas, C. Gattazzo, L.L. Liou, A. Diaspro, J.W. Dossen, E.B. Gralla, and V.D. Longo. 2004. Superoxide is a mediator of an altruistic aging program in *Saccharomyces cerevisiae*. *J. Cell Biol.* 166:1055–1067.

Fabrizio, P., C. Gattazzo, L. Battistella, M. Wei, C. Cheng, K. McGrew, and V.D. Longo. 2005. Sir2 blocks extreme life-span extension. *Cell.* 123:655–667.

Finch, C.E. 1990. Longevity, Senescence, and the Genome. University of Chicago Press, Chicago. 948 pp.

Gangloff, S., J.P. McDonald, C. Bendixen, L. Arthur, and R. Rothstein. 1994. The yeast type I topoisomerase Top3 interacts with Sgs1, a DNA helicase homolog: a potential eukaryotic reverse gyrase. *Mol. Cell. Biol.* 14:8391–8398.

German, J. 1995. Bloom's syndrome. *Dermatol. Clin.* 13:7–18.

Hasty, P., and J. Vijg. 2002. Aging. Genomic priorities in aging. *Science.* 296:1250–1251.

Heidenreich, E., and U. Wintersberger. 1998. Replication-dependent and selection-induced mutations in respiration-competent and respiration-deficient strains of *Saccharomyces cerevisiae*. *Mol. Gen. Genet.* 260:395–400.

Heidenreich, E., R. Novotny, B. Kneidinger, V. Holzmann, and U. Wintersberger. 2003. Non-homologous end joining as an important mutagenic process in cell cycle-arrested cells. *EMBO J.* 22:2274–2283.

Hickson, I.D., S.L. Davies, J.L. Li, N.C. Levitt, P. Mohaghegh, P.S. North, and L. Wu. 2001. Role of the Bloom's syndrome helicase in maintenance of genome stability. *Biochem. Soc. Trans.* 29:201–204.

Johnson, F.B., R.A. Marciniak, M. McVey, S.A. Stewart, W.C. Hahn, and L. Guarente. 2001. The *Saccharomyces cerevisiae* WRN homolog Sgs1p participates in telomere maintenance in cells lacking telomerase. *EMBO J.* 20:905–913.

Kaeberlein, M., R.W. Powers III, K.K. Steffen, E.A. Westman, D. Hu, N. Dang, E.O. Kerr, K.T. Kirkland, S. Fields, and B.K. Kennedy. 2005. Regulation of yeast replicative life span by TOR and Sch9 in response to nutrients. *Science.* 310:1193–1196.

Kaiser, C., S. Michaelis, and A. Mitchell. 1994. Methods in yeast genetics. Cold Spring Harbor Laboratory Press, Cold Spring Harbor, NY. 202 pp.

Kaneko, H., and N. Kondo. 2004. Clinical features of Bloom syndrome and function of the causative gene, BLM helicase. *Expert Rev. Mol. Diagn.* 4:393–401.

Killoran, M.P., and J.L. Keck. 2006. Sit down, relax and unwind: structural insights into RecQ helicase mechanisms. *Nucleic Acids Res.* 34:4098–4105.

Kucsera, J., K. Yarita, and K. Takeo. 2000. Simple detection method for distinguishing dead and living yeast colonies. *J. Microbiol. Methods.* 41:19–21.

Lin, S.J., P.A. Defossez, and L. Guarente. 2000. Requirement of NAD and *SIR2* for life-span extension by calorie restriction in *Saccharomyces cerevisiae. Science.* 289:2126–2128.

Lo, Y.C., K.S. Paffett, O. Amit, J.A. Clikeman, R. Sterk, M.A. Brenneman, and J.A. Nickoloff. 2006. Sgs1 regulates gene conversion tract lengths and crossovers independently of its helicase activity. *Mol. Cell. Biol.* 26:4086–4094.

Lombard, D.B., K.F. Chua, R. Mostoslavsky, S. Franco, M. Gostissa, and F.W. Alt. 2005. DNA repair, genome stability, and aging. *Cell.* 120:497–512.

Longo, V.D. 1997. The pro-senescence role of Ras2 in the chronological life span of yeast. Ph.D. thesis. University of California, Los Angeles, Los Angeles. 41 pp.

Longo, V.D. 2003. The Ras and Sch9 pathways regulate stress resistance and longevity. *Exp. Gerontol.* 38:807–811.

Longo, V.D., and C.E. Finch. 2003. Evolutionary medicine: from dwarf model systems to healthy centenarians. *Science.* 299:1342–1346.

Longo, V.D., E.B. Gralla, and J.S. Valentine. 1996. Superoxide dismutase activity is essential for stationary phase survival in *Saccharomyces cerevisiae*. Mitochondrial production of toxic oxygen species in vivo. *J. Biol. Chem.* 271:12275–12280.

Longo, V.D., L.M. Ellerby, D.E. Bredesen, J.S. Valentine, and E.B. Gralla. 1997. Human Bcl-2 reverses survival defects in yeast lacking superoxide dismutase and delays death of wild-type yeast. *J. Cell Biol.* 137:1581–1588.

Longo, V.D., L.L. Liou, J.S. Valentine, and E.B. Gralla. 1999. Mitochondrial superoxide decreases yeast survival in stationary phase. *Arch. Biochem. Biophys.* 365:131–142.

Madia, F., C. Gattazzo, P. Fabrizio, and V.D. Longo. 2007. A simple model system for age-dependent DNA damage and cancer. *Mech. Ageing Dev.* 128:45–49.

McVey, M., M. Kaeberlein, H.A. Tissenbaum, and L. Guarente. 2001. The short life span of *Saccharomyces cerevisiae* sgs1 and srs2 mutants is a composite of normal aging processes and mitotic arrest due to defective recombination. *Genetics.* 157:1531–1542.

Miyajima, A., M. Seki, F. Onoda, M. Shiratori, N. Odagiri, K. Ohta, Y. Kikuchi, Y. Ohno, and T. Enomoto. 2000a. Sgs1 helicase activity is required for mitotic but apparently not for meiotic functions. *Mol. Cell. Biol.* 20:6399–6409.

Miyajima, A., M. Seki, F. Onoda, A. Ui, Y. Satoh, Y. Ohno, and T. Enomoto. 2000b. Different domains of Sgs1 are required for mitotic and meiotic functions. *Genes Genet. Syst.* 75:319–326.

Mohaghegh, P., and I.D. Hickson. 2002. Premature aging in RecQ helicase-deficient human syndromes. *Int. J. Biochem. Cell Biol.* 34:1496–1501.

Mullen, J.R., V. Kaliraman, and S.J. Brill. 2000. Bipartite structure of the SGS1 DNA helicase in *Saccharomyces cerevisiae*. *Genetics.* 154:1101–1114.

Myung, K., and R.D. Kolodner. 2002. Suppression of genome instability by redundant S-phase checkpoint pathways in *Saccharomyces cerevisiae*. *Proc. Natl. Acad. Sci. USA.* 99:4500–4507.

Myung, K., A. Datta, C. Chen, and R.D. Kolodner. 2001. SGS1, the *Saccharomyces cerevisiae* homologue of BLM and WRN, suppresses genome instability and homeologous recombination. *Nat. Genet.* 27:113–116.

Niedernhofer, L.J., G.A. Garinis, A. Raams, A.S. Lalai, A.R. Robinson, E. Appeldoorn, H. Odijk, R. Oostendorp, A. Ahmad, W. van Leeuwen, et al. 2006. A new progeroid syndrome reveals that genotoxic stress suppresses the somatotroph axis. *Nature.* 444:1038–1043.

Onoda, F., M. Seki, A. Miyajima, and T. Enomoto. 2000. Elevation of sister chromatid exchange in *Saccharomyces cerevisiae* sgs1 disruptants and the relevance of the disruptants as a system to evaluate mutations in Bloom's syndrome gene. *Mutat. Res.* 459:203–209.

Onodera, R., M. Seki, A. Ui, Y. Satoh, A. Miyajima, F. Onoda, and T. Enomoto. 2002. Functional and physical interaction between Sgs1 and Top3 and Sgs1-independent function of Top3 in DNA recombination repair. *Genes Genet. Syst.* 77:11–21.

Ozgenc, A., and L.A. Loeb. 2005. Current advances in unraveling the function of the Werner syndrome protein. *Mutat. Res.* 577:237–251.

Pedrazzi, G., C.Z. Bachrati, N. Selak, I. Studer, M. Petkovic, I.D. Hickson, J. Jiricny, and I. Stagljar. 2003. The Bloom's syndrome helicase interacts directly with the human DNA mismatch repair protein hMSH6. *Biol. Chem.* 384:1155–1164.

Schmidt, K.H., V. Pennaneach, C.D. Putnam, and R.D. Kolodner. 2006. Analysis of gross-chromosomal rearrangements in *Saccharomyces cerevisiae*. *Methods Enzymol.* 409:462–476.

Shen, J.C., and L.A. Loeb. 2000. The Werner syndrome gene: the molecular basis of RecQ helicase-deficiency diseases. *Trends Genet.* 16:213–220.

Sinclair, D.A., K. Mills, and L. Guarente. 1997. Accelerated aging and nucleolar fragmentation in yeast *sgs1* mutants. *Science.* 277:1313–1316.

Spindler, S.R. 2005. Rapid and reversible induction of the longevity, anticancer and genomic effects of caloric restriction. *Mech. Ageing Dev.* 126:960–966.

Sun, H., R.J. Bennett, and N. Maizels. 1999. The *Saccharomyces cerevisiae* Sgs1 helicase efficiently unwinds G-G paired DNAs. *Nucleic Acids Res.* 27:1978–1984.

Thompson, L.H., and D. Schild. 2002. Recombinational DNA repair and human disease. *Mutat. Res.* 509:49–78.

Toda, T., S. Cameron, P. Sass, and M. Wigler. 1988. *SCH9*, a gene of *Saccharomyces cerevisiae* that encodes a protein distinct from, but functionally and structurally related to, cAMP- dependent protein kinase catalytic subunits. *Genes Dev.* 2:517–527.

Ui, A., M. Seki, H. Ogiwara, R. Onodera, S. Fukushige, F. Onoda, and T. Enomoto. 2005. The ability of Sgs1 to interact with DNA topoisomerase III is essential for damage-induced recombination. *DNA Repair (Amst.).* 4:191–201.

Urban, J., A. Soulard, A. Huber, S. Lippman, D. Mukhopadhyay, O. Deloche, V. Wanke, D. Anrather, G. Ammerer, H. Riezman, et al. 2007. Sch9 is a major target of TORC1 in *Saccharomyces cerevisiae*. *Mol. Cell.* 26:663–674.

Vijg, J., and Y. Suh. 2006. Ageing: chromatin unbound. *Nature.* 440:874–875.

Weindruch, R. 1996. The retardation of aging by caloric restriction: studies in rodents and primates. *Toxicol. Pathol.* 24:742–745.

Weindruch, R., and R. Walford. 1988. The Retardation of Aging and Disease by Dietary Restriction. Charles C. Thomas, Springfield, IL. 436 pp.

Yamagata, K., J. Kato, A. Shimamoto, M. Goto, Y. Furuichi, and H. Ikeda. 1998. Bloom's and Werner's syndrome genes suppress hyperrecombination in yeast sgs1 mutant: implication for genomic instability in human diseases. *Proc. Natl. Acad. Sci. USA.* 95:8733–8738.

Yang, Q., R. Zhang, X.W. Wang, S.P. Linke, S. Sengupta, I.D. Hickson, G. Pedrazzi, C. Perrera, I. Stagljar, S.J. Littman, et al. 2004. The mismatch DNA repair heterodimer, hMSH2/6, regulates BLM helicase. *Oncogene.* 23:3749–3756.